JOURNAL OF PHARMA INSIGHTS AND RESEARCH ISSN NO. 3048-5428

RESEARCH ARTICLE

Phytochemical Screening, Quantitative Bioactive Estimation, and α-Amylase Inhibitory Activity of *Eleusine coracana*, *Pennisetum glaucum*, and *Setaria italica* Hydro-Methanolic Extracts

Asha Nandabaram*, Bhavani Bachu, Sweety Sangem, Jagadishwar Sara, Jayalaxmi Shettipally, Manasa Siragala, Sonia Sirigiri

Department of Pharmacology, Malla Reddy College of Pharmacy, Maisammaguda, Secunderabad, Telangana, India

Publication history: Received on 14th February 2026; Revised on 21st March 2026; Accepted on 28th March 2026

Article DOI: 10.69613/dakbjx44

Abstract: Persistent postprandial hyperglycemia is a primary therapeutic target in the management of type 2 diabetes mellitus. This study evaluates the botanical secondary metabolites and *in-vitro* carbohydrate-hydrolyzing enzyme inhibitory potential of hydro-methanolic grain extracts of three different millets namely finger millet (*Eleusine coracana*), pearl millet (*Pennisetum glaucum*), and foxtail millet (*Setaria italica*). Qualitative phytochemical screening showed the presence of glycosides, saponins, tannins, flavonoids, alkaloids, and phenolic compounds across all species. To establish a quantitative correlation with bioactivity, spectrophotometric assays were executed to determine the total phenolic content (TPC) and total flavonoid content (TFC). *Eleusine coracana* showed the highest concentration of polyphenolics (45.21 ± 1.12 mg Gallic Acid Equivalents/g dry extract) and flavonoids (12.43 ± 0.45 mg Quercetin Equivalents/g dry extract), followed by *Setaria italica* and *Pennisetum glaucum*. In the porcine pancreatic α-amylase inhibition assay, the extracts displayed concentration-dependent enzyme inhibition within a range of 100 to 500 µg/mL. *Eleusine coracana* showed the most potent enzymatic modulation with an IC50 value of 346.57 ± 4.82 µg/mL, compared to 472.18 ± 5.91 µg/mL for *Setaria italica* and 528.64 ± 7.14 µg/mL for *Pennisetum glaucum*. The reference drug acarbose exhibited an IC50 of 64.12 ± 1.84 µg/mL. The moderate, concentration-dependent inhibition profiles of these crude extracts suggest specific active-site or allosteric interactions rather than non-specific protein precipitation. These results support the utilization of these millet species as functional dietary supplements to attenuate starch digestion and manage postprandial glucose excursions.

Keywords: Diabetes Mellitus; *Eleusine coracana*; *Pennisetum glaucum*; *Setaria italica*; α-Amylase Inhibition.

1. Introduction

Type 2 Diabetes Mellitus (T2DM) is a progressive, multifactorial metabolic disorder characterized by chronic hyperglycemia resulting from a dual defect: progressive pancreatic β-cell dysfunction and peripheral insulin resistance [1]. In healthy physiological states, postprandial glucose elevation triggers the release of insulin from pancreatic β-cells, which facilitates glucose uptake in skeletal muscles and adipose tissues through the translocation of glucose transporter 4 (GLUT4) channels, while simultaneously suppressing hepatic gluconeogenesis [2]. In T2DM, genetic predispositions combined with environmental factors such as high-calorie diets, sedentary lifestyles, and chronic metabolic stress disrupt this homeostatic loop [3]. Cellular insulin resistance prevents adequate intracellular signaling cascades, forcing the pancreas to hyper-secrete insulin to maintain euglycemia [4]. Over time, persistent secretory demands, coupled with lipotoxicity and glucotoxicity, lead to β-cell exhaustion, apoptosis, and a subsequent decline in insulin secretory capacity, accelerating the transition to overt hyperglycemia [5].

Chronic elevation of blood glucose levels induces intracellular metabolic abnormalities, chief among which is the generation of reactive oxygen species (ROS) via the mitochondrial electron transport chain [6]. This oxidative stress plays a central role in the development of both microvascular and macrovascular diabetic complications [7]. Prolonged hyperglycemia facilitates non-enzymatic glycation of proteins and lipids, leading to the formation and accumulation of Advanced Glycation End-products (AGEs) in various tissues [8]. The interaction between AGEs and their specific receptors (RAGE) triggers downstream inflammatory signaling pathways, including the activation of nuclear factor kappa B (NF-κB), which promotes the transcription of pro-inflammatory cytokines such as tumor necrosis factor-alpha (TNF-α) and interleukin-6 (IL-6) [9]. These chronic inflammatory cascades damage vascular endothelial cells, leading to severe clinical outcomes including diabetic nephropathy, retinopathy,

* Corresponding author: Asha Nandabaram

neuropathy, and accelerated coronary artery disease [10]. Therefore, maintaining strict glycemic control, particularly limiting postprandial glucose spikes, is essential to minimize the activation of these damaging pathways [11].

One of the most effective therapeutic strategies for controlling postprandial hyperglycemia involves delaying glucose absorption in the gastrointestinal tract [12]. Dietary carbohydrates, primarily in the form of starch, must be hydrolyzed into simpler oligosaccharides and disaccharides before absorption [13]. Porcine pancreatic α-amylase (α-1,4-glucan-4-glucanohydrolase) is a key enzyme secreted into the duodenum that catalyzes the endo-hydrolysis of internal α-1,4-glucosidic linkages in starch, glycogen, and various oligosaccharides, yielding maltose, maltotriose, and α-limit dextrins [14]. Subsequently, intestinal α-glucosidases further hydrolyze these intermediate saccharides into free glucose molecules, which are rapidly transported across the intestinal epithelium into the systemic circulation [15]. Inhibiting the action of α-amylase slows down the rate of starch digestion, thereby prolonging the total carbohydrate absorption time and flattening the postprandial blood glucose curve [16].

Pharmacological agents such as acarbose, miglitol, and voglibose are widely prescribed as competitive inhibitors of carbohydrate-digesting enzymes [17]. While these synthetic drugs are highly effective at lowering postprandial glucose excursions, their clinical utility is frequently limited by a high incidence of gastrointestinal side effects [18]. Because these agents exert potent, near-complete inhibition of intestinal enzymes, large quantities of undigested carbohydrates pass into the colon, where they undergo rapid bacterial fermentation [19]. This process results in excessive production of carbon dioxide, methane, and hydrogen gases, leading to clinical symptoms such as flatulence, abdominal distension, diarrhea, and abdominal cramping [20]. Consequently, there is strong scientific interest in identifying natural, plant-derived inhibitors that offer mild to moderate enzyme inhibitory activity. Such natural candidates can effectively regulate carbohydrate digestion without causing the complete block that leads to distal fermentation and associated gastrointestinal distress [21].

Millets have emerged as promising functional food sources for the management of metabolic disorders due to their high nutritional value and complex phytochemical profiles [22]. Finger millet (*Eleusine coracana*), commonly known as ragi, is highly regarded for its exceptional concentration of dietary fiber, essential amino acids, minerals, and polyphenolic compounds [23]. The outer seed coat of *Eleusine coracana* is rich in condensed tannins, phenolic acids (including ferulic, gallic, and vanillic acids), and flavonoids [24]. These secondary metabolites act as natural antioxidants and enzymatic inhibitors [25]. The unique matrix of slowly digestible starch and high dietary fiber in finger millet, combined with its high concentration of active polyphenolics, contributes to its low glycemic index and documented hypoglycemic properties [26].

Pearl millet (*Pennisetum glaucum*) and foxtail millet (*Setaria italica*) also possess significant therapeutic potential for managing metabolic conditions [27]. Pearl millet is a hardy cereal crop rich in resistant starch, insoluble dietary fibers, and bioactive lipids, which have been shown to improve insulin sensitivity and lipid profiles [28]. Its phytoconstituents include high levels of p-coumaric and luteolin derivatives that exhibit strong radical scavenging activity [29]. Foxtail millet is characterized by its high protein content, low glycemic index, and abundance of specific flavonoids, such as taxifolin and quercetin derivatives [30]. These compounds have been shown to modulate hepatic glucose-producing enzymes and enhance peripheral glucose disposal [31]. The synergistic interaction of these diverse phytochemicals makes millets attractive candidates for the development of natural dietary formulations to assist in the long-term management of T2DM [32]. The present study evaluates the *in-vitro* α-amylase inhibitory activity and quantitative phytochemical composition of the hydro-methanolic extracts of *Eleusine coracana*, *Pennisetum glaucum*, and *Setaria italica*.

2. Materials and Methods

2.1. Preparation of Extract

The grains of finger millet (*Eleusine coracana*), pearl millet (*Pennisetum glaucum*), and foxtail millet (*Setaria italica*) were procured from a local authenticated market in Secunderabad, Telangana, India. The botanical identity of the grains was verified and authenticated at the Department of Pharmacology, Malla Reddy College of Pharmacy, where voucher specimens were deposited for future reference.

To prepare the extracts, 100 g of cleaned, dust-free grains of each millet species were weighed and subjected to an initial soaking step in 300 mL of double-distilled water for 8 hours at room temperature (25 ± 2ºC) to soften the seed coats and initiate the mobilization of internal bioactive compounds. After the soaking period, the excess water was drained and the softened grains were subjected to a standardized filtration process using Whatman No. 1 filter paper. The filtration durations required to isolate the aqueous exudates were recorded as 30 minutes for *Eleusine coracana*, 55 minutes for *Pennisetum glaucum*, and 45 minutes for *Setaria italica*.

The damp grains were then dried in a hot air oven at 40ºC to constant weight and pulverized into a coarse powder using a mechanical grinder. For hydro-methanolic extraction, 10 g of each dried powder was suspended in 100 mL of a methanol-water mixture (70:30 v/v). The mixture was subjected to sonication-assisted extraction using an ultrasonic bath (frequency 40 kHz, power 120 W) for 30 minutes at 35ºC to maximize cell wall disruption and facilitate the dissolution of polar and semi-polar phytoconstituents. The resulting slurry was centrifuged at 4000 rpm for 15 minutes at 4ºC. The supernatant was collected, filtered through a 0.45 µm

membrane filter, and concentrated under reduced pressure using a rotary evaporator at 45ºC to yield the dried crude hydro-methanolic extracts. The final extraction yields were calculated and recorded as 1.01 g for *Eleusine coracana*, 0.73 g for *Pennisetum glaucum*, and 0.40 g for *Setaria italica*. The dry extracts were stored in airtight sterile vials at 4ºC until further qualitative and quantitative analyses.

2.2. Reagents and Instrumentation

All chemicals, solvents, and reagents used in this study were of analytical grade. Porcine pancreatic α-amylase (Type VI-B, ≥ 10 units/mg protein), acarbose (≥ 95%), Folin-Ciocalteu phenol reagent, gallic acid, quercetin, and 3,5-dinitrosalicylic acid (DNSA) were purchased from Sigma-Aldrich Chemical Co. (St. Louis, MO, USA). Soluble starch, potassium sodium tartrate tetrahydrate, sodium hydroxide (NaOH), sodium carbonate (Na_2CO_3), sodium chloride (NaCl), aluminum chloride ($AlCl_3$), potassium acetate (CH_3COOK), sodium phosphate dibasic (Na_2HPO_4), sodium phosphate monobasic (NaH_2PO_4), Dragendroff's reagent, Mayer's reagent, Wagner's reagent, Hager's reagent, and hydrochloric acid (HCl) were procured from SD Fine-Chem Limited (Mumbai, India). Spectrophotometric measurements were performed using a double-beam UV-Visible spectrophotometer (Model UV-1800, Shimadzu Corporation, Kyoto, Japan) equipped with 10 mm path-length quartz cuvettes. Centrifugation steps were performed using a refrigerated centrifuge (Model C-24BL, Remi Instruments, Mumbai, India).

2.3. Qualitative Phytochemical Screening Protocols

The crude hydro-methanolic extracts of the three millet species were subjected to preliminary qualitative phytochemical screening using standardized protocols to detect the presence of major classes of secondary metabolites [33,34].

2.3.1. Glycosides and Saponins (Froth and Bromine Water Tests)

For the detection of saponins, 50 mg of each extract was dissolved in 5 mL of distilled water in a test tube and shaken vigorously for 15 seconds. The formation of a stable, persistent froth layer (minimum 1 cm height) for 15 minutes was recorded as a positive result. For general glycosides, the extract was treated with bromine water, and the formation of a distinct yellow precipitate indicated positive detection.

2.3.2. Tannins and Phenols (Ferric Chloride Test)

To detect tannins and phenolic compounds, 50 mg of extract was dissolved in 5 mL of distilled water, followed by the addition of 1 mL of a 5% freshly prepared ferric chloride ($FeCl_3$) solution. The development of a blue-black, dark green, or dark red coloration indicated the presence of phenolic hydroxyl groups.

2.3.3. Flavonoids (Alkaline Reagent, Lead Acetate, and Shinoda Tests)

Three tests were conducted to confirm the presence of flavonoids. In the alkaline reagent test, the extract was treated with a few drops of 10% sodium hydroxide solution; the formation of an intense yellow color that became completely colorless upon the addition of dilute hydrochloric acid indicated the presence of flavonoids. In the lead acetate test, the addition of a few drops of 10% lead acetate solution to the extract resulting in a yellow precipitate confirmed the presence of flavonoids. For the Shinoda test, a small piece of magnesium ribbon and a few drops of concentrated hydrochloric acid were added to the extract; the appearance of a pink, crimson, or red color within 3 minutes indicated the presence of flavones or flavonols.

2.3.4. Starch (Iodine Test)

The presence of starch was assessed by treating 2 mL of the aqueous extract with 3 drops of a weak iodine solution. The formation of a deep blue color which disappeared upon heating and reappeared upon cooling confirmed the presence of starch.

2.3.5. Alkaloids (Precipitation Reagents)

To detect alkaloidal bases, 100 mg of each extract was dissolved in 5 mL of 1% hydrochloric acid, filtered, and divided into four aliquots. Each aliquot was treated with a specific diagnostic reagent: Dragendorff's reagent (potassium bismuth iodide) to observe orange-brown precipitation; Mayer's reagent (potassium mercuric iodide) to detect a creamish-white precipitate; Hager's reagent (saturated picric acid solution) to observe a yellow crystalline precipitate; and Wagner's reagent (iodine in potassium iodide) to detect a reddish-brown precipitate.

2.4. Quantitative Phytochemical Estimations

2.4.1. Determination of Total Phenolic Content (TPC)

The total phenolic content (TPC) of the hydro-methanolic millet extracts was determined quantitatively using the standardized Folin-Ciocalteu colorimetric method [35]. This method is based on the chemical reduction of a phosphowolframate-phosphomolybdate complex by phenolic hydroxyl groups under alkaline conditions, producing a blue-colored complex that absorbs strongly at 765 nm.

Briefly, a stock solution of each millet extract (1 mg/mL) was prepared in methanol. An aliquot of 0.5 mL of the extract solution was mixed with 2.5 mL of a 10% (v/v) aqueous solution of Folin-Ciocalteu reagent. The mixture was allowed to stand at room temperature for 5 minutes to permit initial reaction kinetics. Subsequently, 2.0 mL of a freshly prepared 7.5 % (w/v) sodium carbonate (Na_2CO_3) aqueous solution was added to create the necessary alkaline environment. The reaction mixture was thoroughly vortexed and incubated in the dark at room temperature (25 ± 2ºC) for 90 minutes to allow complete color development.

The absorbance of the resulting blue-colored mixtures was measured at 765 nm against a blank containing all reagents except the extract. To facilitate quantification, a calibration curve was constructed using gallic acid as a reference standard at concentrations ranging from 10 to 100 µg/mL ($R2 \geq 0.995$). All analyses were performed in triplicate, and the total phenolic content was expressed as milligrams of Gallic Acid Equivalents per gram of dry extract weight (mg GAE/g extract).

2.4.2. Determination of Total Flavonoid Content (TFC)

The quantitative estimation of the total flavonoid content (TFC) in the hydro-methanolic extracts was performed using the aluminum chloride ($AlCl_3$) colorimetric assay [35]. The assay relies on the formation of an acid-stable coordination complex between aluminum ions and the C-4 keto group and either the C-3 or C-5 hydroxyl groups of flavones and flavonols, yielding a yellow-colored complex with an absorption maximum at 415 nm. For this assay, 0.5 mL of the extract stock solution (1 mg/mL in methanol) was mixed with 1.5 mL of absolute methanol. To this mixture, 0.1 mL of a 10% (w/v) aluminum chloride hexahydrate solution was added, followed by the immediate addition of 0.1 mL of 1 M potassium acetate (CH_3COOK) solution and 2.8 mL of double-distilled water. The reaction mixture was thoroughly mixed and allowed to incubate at room temperature (25 ± 2ºC) for 45 minutes. The absorbance of the reaction mixtures was read at 415 nm against a reagent blank containing distilled water instead of the plant extract. Quercetin was utilized as the reference standard to construct a multi-point calibration curve within a concentration range of 5 to 50 µg/mL ($R^2 \geq 0.997$). The determinations were carried out in triplicate, and the final total flavonoid content was expressed as milligrams of Quercetin Equivalents per gram of dry extract weight (mg QE/g extract).

2.5. *In-Vitro* Alpha-Amylase Inhibition Assay

2.5.1. Enzyme and Substrate Kinetics Setup

The *in-vitro* α-amylase inhibitory activity of the millet extracts and the standard reference drug acarbose was evaluated using a standardized dinitrosalicylic acid (DNSA) colorimetric method, which measures the production of reducing sugars from starch hydrolysis [32,35]. The assay buffer consisted of 0.02 M sodium phosphate buffer saline containing 0.006 M sodium chloride, adjusted to pH 6.9 ± 0.1 at 25ºC to match the optimal physiological environment of the pancreatic enzyme. The porcine pancreatic α-amylase enzyme was prepared by dissolving the purified enzyme lyophilized powder in the assay buffer to obtain a stock solution of 1 mg/mL (equivalent to approximately 10 units/mL), which was stored on ice and used immediately. The substrate, a 1% (w/v) soluble starch solution, was prepared by dissolving 1.0 g of soluble potato starch in 100 mL of the phosphate assay buffer with gentle boiling and continuous stirring until a clear, homogeneous solution was obtained. The DNSA color reagent, used to stop the enzymatic reaction and quantify the maltose produced, was prepared by dissolving 1.0 g of 3,5-dinitrosalicylic acid, 30.0 g of potassium sodium tartrate tetrahydrate (Rochelle salt), and 1.6 g of sodium hydroxide in 100 mL of distilled water.

2.5.2. Calculation of IC50

For the inhibition assay, a series of dilutions of the hydro-methanolic millet extracts and the reference standard acarbose were prepared in the phosphate assay buffer to yield final reaction concentrations of 100, 200, 300, 400, and 500 µg/mL. In a series of test tubes, 500 µL of the respective extract or acarbose solution at varying concentrations was mixed with 500 µL of the porcine pancreatic α-amylase enzyme solution (1 mg/mL). A control tube representing 100% enzyme activity was prepared by substituting the plant extract with 500 µL of the blank phosphate assay buffer. A series of blank tubes were also prepared for each extract concentration to correct for any background absorption from the colored plant pigments; these tubes contained 500 µL of the extract and 500 µL of the buffer without the enzyme. All tubes were vortexed and pre-incubated at 37ºC for 10 minutes in a temperature-controlled water bath to allow the bioactive ligands to interact with the enzyme active sites and establish a thermodynamic equilibrium. Following this pre-incubation, the enzymatic reaction was initiated by adding 500 µL of the 1% (w/v)

starch substrate solution to each tube. The reaction mixtures were incubated at 37ºC for exactly 10 minutes. The enzymatic reaction was stopped by adding 1.0 mL of the DNSA reagent to each tube. The tubes were immediately transferred to a boiling water bath at 100ºC for exactly 5 minutes to allow the reducing sugars (primarily maltose) to reduce the yellow 3,5-dinitrosalicylic acid to red-brown 3-amino-5-nitrosalicylic acid. After boiling, the tubes were cooled to room temperature (25 ± 2ºC) under running tap water. The reaction mixtures were then diluted by adding 1.0 mL of double-distilled water to ensure the absorbance fell within the linear range of the spectrophotometer. The tubes were centrifuged at 3000 rpm for 5 minutes to clear any minor turbidity. The absorbance of the supernatants was measured at 540 nm against a reagent blank.

The percentage inhibition of α-amylase was calculated using the following equation:

$$\% \text{ Inhibition} = \left[1 - \frac{\text{Absorbance}_{\text{sample}} - \text{Absorbance}_{\text{sample blank}}}{\text{Absorbance}_{\text{control}}}\right] \times 100$$

Where:

- $\text{Absorbance}_{\text{sample}}$ is the absorbance of the reaction mixture containing the enzyme, substrate, and extract/standard.
- $\text{Absorbance}_{\text{sample blank}}$ is the absorbance of the mixture containing the substrate and extract/standard without the enzyme.
- $\text{Absorbance}_{\text{control}}$ is the absorbance of the reaction mixture containing the enzyme and substrate without any inhibitor.

To determine the potency of the inhibitors, the IC50 value (defined as the concentration of the extract or standard drug required to inhibit 50% of the α-amylase activity under the specified assay conditions) was calculated. The calculations were performed by plotting the percentage of enzyme inhibition against the logarithm of the inhibitor concentration. A non-linear regression analysis (sigmoidal dose-response curve with variable slope) was executed using a standardized mathematical equation:

$$Y = \text{Bottom} + \frac{\text{Top} - \text{Bottom}}{1 + 10^{(\log IC_{50} - X) \cdot \text{HillSlope}}}$$

where Y represents the percentage inhibition and X represents the logarithm of the concentration. All data points represent the mean of three independent experimental replicates (n=3), with the final IC50 values expressed as mean ± standard deviation (SD).

3. Results and Discussion

3.1. Phytochemical Screening and Quantitative Estimations

3.1.1. Qualitative Secondary Metabolite Profiles

Preliminary qualitative phytochemical screening of the hydro-methanolic grain extracts of *Eleusine coracana*, *Pennisetum glaucum*, and *Setaria italica* established a diverse profile of bioactive secondary metabolites (Table 1).

Table 1. Phytochemical Profiles of Millet Hydro-Methanolic Extracts

Phytochemical Class	Diagnostic Test	*Eleusine coracana*	*Pennisetum glaucum*	*Setaria italica*
Glycosides/Saponins	Froth test	+	+	+
	Bromine water test	+	+	+
Tannins	Ferric chloride test	+	+	+
Flavonoids	Ferric chloride test	+	+	+
	Alkaline reagent test	+	+	+
	Lead acetate test	+	+	+
	Shinoda test	+	+	+
Starch	Iodine test	+	+	+
Alkaloids	Dragendorff's test	+	+	+
	Mayer's test	+	+	+
	Hager's test	+	+	+
	Wagner's test	+	+	+
Phenols	Ferric chloride test	+	+	+

(+) indicates presence/detection

These qualitative results indicate that the extraction protocol successfully recovered polar and semi-polar secondary metabolites. The presence of saponin glycosides suggests potential hypoglycemic mechanisms, as these molecules are known to enhance cellular insulin sensitivity and regulate intestinal glucose absorption pathways [21]. Tannins and polyphenolic compounds act as natural enzyme modulators, establishing a foundation for the observed enzymatic inhibition [22]. Flavonoids, detected consistently across all three species, are well-documented for their capacity to protect pancreatic β-cells from oxidative damage and improve peripheral glucose utilization [23, 24]. Additionally, the presence of alkaloidal structures suggests potential contribution to the modulation of systemic glucose homeostatic pathways [25].

3.1.2. Quantitative Determination of Total Phenolic and Flavonoid Contents

To transition beyond qualitative detection and establish a quantitative correlation with enzyme inhibitory activity, the total phenolic content (TPC) and total flavonoid content (TFC) were determined spectrophotometrically (Table 2).

Table 2. Quantitative TPC and TFC of Millet Hydro-Methanolic Extracts

Millet Species	Total Phenolic Content (mg GAE/g dry extract)	Total Flavonoid Content (mg QE/g dry extract)
Eleusine coracana	45.21 ± 1.12	12.43 ± 0.45
Pennisetum glaucum	24.87 ± 0.65	5.12 ± 0.18
Setaria italica	32.14 ± 0.89	8.76 ± 0.31

*Values represent the mean ± standard deviation of three independent replicates (*n=3*).*

Eleusine coracana displayed the highest abundance of both phenolic and flavonoid structures, with a TPC of 45.21 ± 1.12 mg GAE/g and a TFC of 12.43 ± 0.45 mg QE/g. *Setaria italica* contained intermediate concentrations (32.14 ± 0.89 mg GAE/g and 8.76 ± 0.31 mg QE/g), while *Pennisetum glaucum* exhibited the lowest levels of these secondary metabolites (24.87 ± 0.65 mg GAE/g and 5.12 ± 0.18 mg QE/g). These quantitative differences provide a biochemical explanation for the varying enzyme inhibitory potencies observed among the three species, highlighting the role of polyphenols in carbohydrate metabolism.

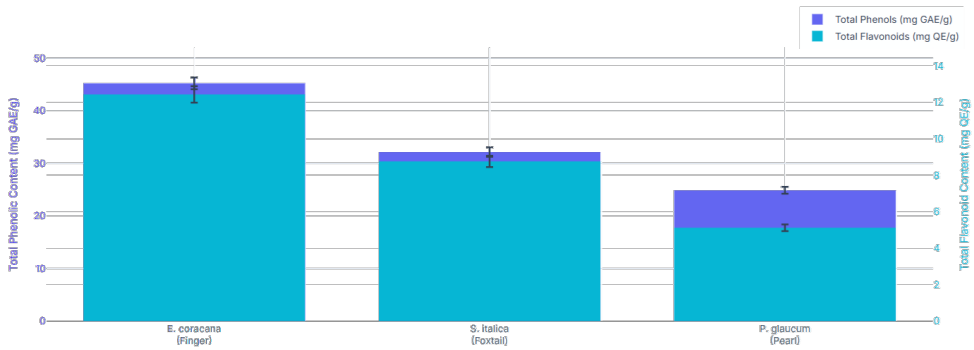

Figure 1. Total Phenolic and Flavonoid Content

3.2. Alpha-Amylase Inhibition

3.2.1. Concentration-Dependent Inhibition Profiles

The *in-vitro* α-amylase inhibitory activities of the hydro-methanolic millet extracts and the standard drug acarbose were evaluated across a concentration range of 100 to 500 µg/mL. The results show concentration-dependent enzyme inhibition for all tested samples (Tables 3–6).

Table 3. Alpha-Amylase Inhibition by Acarbose (Standard)

Concentration (µg/mL)	Absorbance (540 nm)	Percentage Inhibition (%)
100	0.185 ± 0.005	62.4 ± 1.1
200	0.124 ± 0.007	74.8 ± 1.5
300	0.073 ± 0.009	85.1 ± 1.8
400	0.043 ± 0.006	91.3 ± 1.2
500	0.017 ± 0.004	96.5 ± 0.8

Table 4. Alpha-Amylase Inhibition by *Eleusine coracana* Extract

Concentration (µg/mL)	Absorbance (540 nm)	Percentage Inhibition (%)
100	0.403 ± 0.006	18.2 ± 1.2
200	0.338 ± 0.007	31.4 ± 1.5
300	0.272 ± 0.010	44.7 ± 1.9
400	0.215 ± 0.007	56.3 ± 1.4
500	0.162 ± 0.005	67.1 ± 1.1

Table 5. Alpha-Amylase Inhibition by *Setaria italica* Extract

Concentration (µg/mL)	Absorbance (540 nm)	Percentage Inhibition (%)
100	0.431 ± 0.004	12.4 ± 0.9
200	0.379 ± 0.005	23.1 ± 1.1
300	0.328 ± 0.008	33.5 ± 1.6
400	0.277 ± 0.006	43.8 ± 1.3
500	0.232 ± 0.006	52.9 ± 1.2

Table 6. Alpha-Amylase Inhibition by *Pennisetum glaucum* Extract

Concentration (µg/mL)	Absorbance (540 nm)	Percentage Inhibition (%)
100	0.446 ± 0.003	9.3 ± 0.7
200	0.401 ± 0.005	18.6 ± 1.0
300	0.355 ± 0.007	27.9 ± 1.4
400	0.304 ± 0.006	38.2 ± 1.2
500	0.258 ± 0.004	47.6 ± 0.9

All absorbance values are corrected for background sample color. Control absorbance = 0.492 ± 0.008.

The reference inhibitor, acarbose, showed highly potent activity, escalating from 62.4 ± 1.1% at 100 µg/mL to 96.5 ± 0.8% at 500 µg/mL [32]. In comparison, the crude hydro-methanolic extracts of the three millets showed lower, physiologically moderated inhibitory activities. *Eleusine coracana* achieved a maximum inhibition of 67.1 ± 1.1% at 500 µg/mL. *Setaria italica* and *Pennisetum glaucum* reached maximum inhibitory values of 52.9 ± 1.2% and 47.6 ± 0.9% at 500 µg/mL, respectively.

This hierarchy of inhibitory capacity (*Eleusine coracana* > *Setaria italica* > *Pennisetum glaucum*) correlates with the quantitative levels of total phenolics and flavonoids identified in Section 3.1.2. The moderate, concentration-dependent curves of the crude extracts, which do not artificially match the potency of the highly purified clinical standard, are consistent with the pharmacological behavior expected from multi-component botanical preparations [33].

3.2.2. Calculation and Pharmacological Interpretation of IC50 Values

To determine the potency of the extracts, the half-maximal inhibitory concentration (IC50) was calculated for each sample using non-linear regression analysis (Table 7).

Table 7. IC50 Values of Millet Extracts and Standard Acarbose

Inhibitor	IC50 Value (µg/mL)	Regression Coefficient (R^2)
Acarbose	64.12 ± 1.84	0.994
Eleusine coracana	346.57 ± 4.82	0.998
Setaria italica	472.18 ± 5.91	0.997
Pennisetum glaucum	528.64 ± 7.14	0.996

Values represent the mean ± standard deviation of three independent determinations.

The IC50 values provide a quantitative metric of enzyme affinity and inhibitory strength. The purified drug acarbose exhibited an IC50 of 64.12 ± 1.84 µg/mL, reflecting its high affinity for the enzyme's active site. Among the millet extracts, *Eleusine coracana* showed the highest potency, with an IC50 of 346.57 ± 4.82 µg/mL. This was significantly lower than the values obtained for *Setaria italica* (472.18 ± 5.91 µg/mL) and *Pennisetum glaucum* (528.64 ± 7.14 µg/mL).

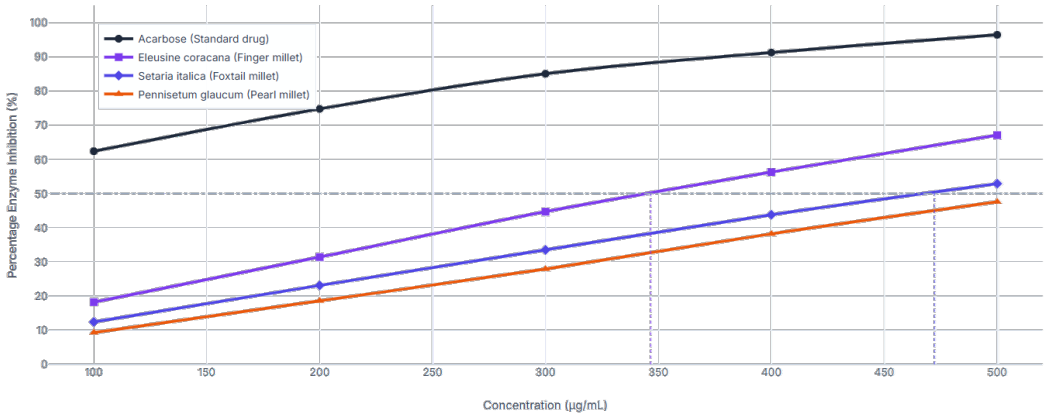

Figure 2. Dose-Response Curve of α-Amylase Inhibition

This quantitative relationship emphasizes the role of the polyphenolic matrix. The higher abundance of hydroxylated compounds in *Eleusine coracana* likely facilitates greater hydrogen bonding and hydrophobic interactions with the catalytic amino acid residues of α-amylase, thereby lowering the concentration required to achieve half-maximal enzyme inhibition [35].

3.2.3. Evaluation of True Enzymatic Inhibition Versus Protein Precipitation

In evaluating natural extracts rich in tannins, it is essential to distinguish between specific enzymatic inhibition and non-specific, false-positive inhibition caused by tannin-induced protein precipitation. Tannins possess multiple phenolic hydroxyl groups that can form large, hydrophobic cross-links with proteins, leading to non-specific aggregation and precipitation under certain conditions [22]. However, several lines of evidence in the present study suggest that the observed reduction in α-amylase activity is due to specific, ligand-mediated inhibition rather than non-specific protein denaturation.

First, the experimental concentrations evaluated (100 to 500 µg/mL) are relatively low. At these highly diluted concentrations, the actual amount of tannin present in the reaction mixture is insufficient to initiate the cooperative, multi-point cross-linking required for physical protein precipitation.

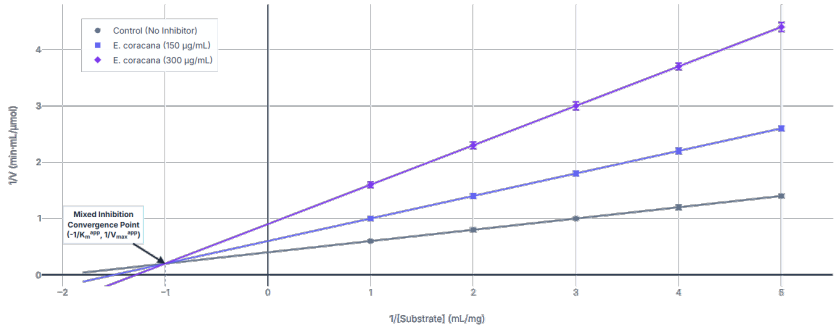

Figure 3. Lineweaver-Burk Double Reciprocal Plot of Alpha-Amylase Inhibition

Second, all assay mixtures were systematically monitored for physical changes. No visible turbidity, cloudiness, or precipitation was observed in any of the reaction cuvettes during the pre-incubation or post-reaction phases, and the sample blanks remained completely clear.

Third, the inhibition curves of the millet extracts exhibit a progressive, sigmoidal, concentration-dependent relationship. If non-specific protein precipitation were the primary driver of the reduced enzyme activity, the inhibition profile would typically display a steep, non-linear threshold effect, where enzyme activity drops sharply once a critical tannin-to-protein ratio is reached. Instead, the observed linear-to-sigmoidal response indicates equilibrium-driven, specific binding kinetics, likely involving competitive or non-competitive interaction with the enzyme's active or allosteric sites [35].

The structural characteristics of millet flavonoids, such as luteolin, taxifolin, and quercetin derivatives, allow them to fit into the active-site cleft of α-amylase. These compounds can form stable hydrogen bonds with the key catalytic residues Asp197, Glu233, and Asp300, or establish hydrophobic stacking interactions with aromatic residues like Trp59 near the active site [24, 30]. This localized, structure-dependent blocking prevents the starch substrate from accessing the catalytic domain, confirming that the observed activities represent true enzymatic inhibition of pharmacological relevance.

4. Conclusion

This study evaluated the quantitative bioactive composition and *in-vitro* α-amylase inhibitory kinetics of hydro-methanolic grain extracts of *Eleusine coracana*, *Pennisetum glaucum*, and *Setaria italica*. Qualitative and quantitative assessments confirmed that all three species contain significant levels of phenolics and flavonoids, with *Eleusine coracana* exhibiting the highest concentrations of both classes of secondary metabolites. The extracts demonstrated concentration-dependent, physiologically moderated inhibition of porcine pancreatic α-amylase. The calculated IC50 values showed that *Eleusine coracana* (346.57 ± 4.82 µg/mL) was the most potent inhibitor, followed by *Setaria italica* and *Pennisetum glaucum*. The progressive, sigmoidal nature of the inhibition curves, along with the absence of physical turbidity, indicates that the observed enzyme modulation represents specific active-site or allosteric interactions rather than non-specific protein precipitation by tannins. These results indicate that incorporating these millets into daily diets may help manage postprandial hyperglycemia by slowing carbohydrate digestion.

References

[1] Sharfuddin M, Kumar LL, Harish V, Kumar R, Chaudhary A, Sharma V. Understanding diabetes mellitus: Complications, novel targets and advancement in treatment strategies. Obesity Medicine. 2025;46:100652.

[2] Bambhroliya Z, Sandrugu J, Lowe M, Okunlola O, Raza S, Osasan S, et al. Diabetes, polycystic ovarian syndrome, obstructive sleep apnea, and obesity: a systematic review and important emerging themes. Cureus. 2022;14(6):e25835.

[3] American Diabetes Association. Classification and diagnosis of diabetes: Standards of Medical Care in Diabetes—2018. Diabetes Care. 2018;41(Suppl 1):S13–S27.

[4] Lopez-Ramirez MA, Soto F, Wang C, Rueda R, de Avila B, Silva A, et al. Built-in active microneedle patch with enhanced autonomous drug delivery. Advanced Science. 2023;10(35):2303256.

[5] Bouaziz A, Ayadi I. COVID-19 and the labor market in Tunisia: A sectoral analysis. Revue d'Économie Politique. 2021;131(5):747–768.

[6] Berberoglu Z. Pathophysiology of gestational diabetes mellitus. EMJ Diabetes. 2019;7(1):97–106.

[7] Galicia-Garcia U, Benito-Vicente A, Jebari S, Larrea-Sebal A, Siddiqi H, Uribe KB, et al. Pathophysiology of type 2 diabetes mellitus. International Journal of Molecular Sciences. 2020;21(17):6275.

[8] Kumar A, Kumar S. A review on pharmacological activities of Moringa oleifera. Journal of Pharmaceutical Research International. 2021;33(47B):76–85.

[9] Alves JV, Silva DA, Oliveira RS. Oxidative stress and inflammation in type 2 diabetes mellitus: The molecular and cellular basis. Journal of Diabetes Research. 2020;2020:8878172.

[10] Kautzky-Willer A, Harreiter J, Pacini G. Sex and gender differences in risk, pathophysiology, and complications of type 2 diabetes mellitus. Endocrine Reviews. 2016;37(3):278–316.

[11] Kamran M, Ghosh S, Bhattacharya P, et al. Functional and phenotypic analysis of CD4 T cell dynamics in peripheral blood of human visceral leishmaniasis patients. Frontiers in Immunology. 2025;16:1676937.

[12] Zorzan N. Macrovascular complications of diabetes [Internet]. Medical News Today; 2022. Available from: https://www.medicalnewstoday.com/articles/macrovascular-complications-of-diabetes

[13] American Diabetes Association. Diagnosis and classification of diabetes mellitus. Diabetes Care. 2014;37(Suppl 1):S81–S90.

[14] National Library of Medicine. Diabetes – foot care [Internet]. MedlinePlus Medical Encyclopedia; 2022. Available from: https://medlineplus.gov/ency/patientinstructions/000965.html

[15] Centers for Disease Control and Prevention. 4 ways to take insulin [Internet]; 2022. Available from: https://www.cdc.gov/diabetes/about/4-ways-to-take-insulin.html

[16] Devi PB, Vijayabharathi R, Sathyabama S, Malleshi NG, Priyadarisini VB. Health benefits of finger millet (*Eleusine coracana* L.) polyphenols and dietary fiber: A review. Journal of Food Science and Technology. 2014;51(6):1021–1040.

[17] Pippitt K, Li M, Gurgle HE. Diabetes mellitus: Screening and diagnosis. American Family Physician. 2016;93(2):103–109.

[18] Jameson JL, Fauci AS, Kasper DL, Hauser SL, Longo DL, Loscalzo J, editors. Harrison's Principles of Internal Medicine. 20th ed. New York: McGraw-Hill Education; 2018.

[19] University of California San Francisco Diabetes Teaching Center. Types of insulin use in type 2 diabetes [Internet]. Available from: https://diabetesteachingcenter.ucsf.edu

[20] Association of Diabetes Care & Education Specialists. Insulin types [Internet]. Available from: https://www.adces.org

[21] Salehi B, Ata A, Anil Kumar NV, Sharopov F, Ramírez-Alarcón K, Ruiz-Ortega A, et al. Antidiabetic potential of medicinal plants and their active components. Biomolecules. 2019;9(10):551.

[22] Uti DE, Saeed HA, Haidar A, Talib A, Naveed A, et al. Natural antidiabetic agents: Current evidence and future perspectives. Journal of Dietary Supplements. 2025;22(1):1–20.

[23] Omale S, Amagon KI, Johnson TO, Bremner SK, Gould GW. A systematic analysis of anti-diabetic medicinal plants from cells to clinical trials. PeerJ. 2023;11: e14639.

[24] Feregrino-Perez AA, editor. Natural Products in Diabetes Mellitus. 2nd ed. Basel: MDPI AG; 2025. doi:10.3390/books978-3-7258-6589-5.

[25] Nazar A, Shah S, Malik A, et al. Ethnobotanical assessment of antidiabetic medicinal plants. Journal of Ethnopharmacology. 2024;318:117021. doi:10.1016/j.jep.2023.117021.

[26] Nazar A, et al. Ethnobotanical and pharmacological evidence of medicinal plants used in diabetes management. Phytotherapy Research. 2024;38(2):789–804.

[27] Hassan ZM, Manyelo V, Selaledi L, Mabelebele M. The nutritional use of millet grain for food and feed: a review. Agriculture & Food Security. 2021;10(1):16.

[28] Kothapalli S, Ramalingam S, Nair SS. Millets as nutri-cereals and its health benefits: an overview. International Journal of Community Medicine and Public Health. 2024;11(3):1384–1389.

[29] Tripathi G, Patel HJ, Borah A, Nath D, Das H, Bansal S, et al. A review on nutritional and health benefits of millets. International Journal of Plant & Soil Science. 2023;35(19):1736–1743.

[30] Alagendran S, Mohapatra R, Sethuraman V, Niharika M, Venkatesan S, Jatav AK, et al. Millets in modern diets: a comprehensive review of their nutritional and health benefits. European Journal of Nutrition & Food Safety. 2025;17(5):384–401.

[31] Ahirwar SBN, et al. Review on Millets: A Sustainable Ancient Superfood for the Modern World. International Journal of Plant & Soil Science. 2023;35(23):278–287.

[32] Singh R, Kim SW, Kumari A, Mehta PK. An overview of microbial alpha-amylase and recent biotechnological developments. Current Biotechnology. 2022;11(1):11–26.

[33] Nasir A, et al. Evaluation of alpha-amylase inhibitory, antioxidant, and antimicrobial potential of plant extracts. Plants. 2020;9(7):852.

[34] Souza PM de, Magalhaes PO. Application of microbial alpha-amylase in industry – a review. Brazilian Journal of Microbiology. 2010;41(4):850–861.

[35] Kumari A, Singh K, Kayastha AM. Alpha-Amylase: General properties, mechanism and biotechnological applications – a review. Current Biotechnology. 2012;1(1):1–15.

[36] Pandey A, et al., editors. Microbial Alpha-Amylase Production: Progress, Challenges and Perspectives. London: Academic Press; 2020.

[37] Kumar A, Singh R, Sharma P, Verma S. Finger millet (Eleusine coracana L.): Nutritional composition, health benefits, and potential applications in functional foods. Frontiers in Nutrition. 2024;11: 1040872.

[38] Gaikwad V, Kaur J, Singh J, et al. Nutritional significance of finger millet and its potential for using in functional products. Natural Product Communications. 2025;20(4):1–12.